ISSN: 2447-3359

REVISTA DE GEOCIÊNCIAS DO NORDESTE

Northeast Geosciences Journal

v. 11, nº 1 (2025)

https://doi.org/10.21680/2447-3359.2025v11n1ID38735

Residual topographic modeling (RTM) effect associated with lateral density variation in Brazil

Efeito residual da modelagem topográfica (RTM) associado à variação da densidade lateral no Brasil

Roosevelt De Lara Santos Junior.[1]

[1] Federal University of Rio Grande do Sul (UFRGS), Institute of Geosciences, Department of Geodesy, Porto Alegre/RS, Brazil. Email: rooseveltdelara@ufrgs.br
ORCID: https://orcid.org/0000-0003-4390-8636

Abstract: This study presents three representations of the behavior of Residual Topographic Modeling (RTM) covering the entire continental territory of Brazil, using global lateral density models UNB_TopoDens and CRUST 1.0 (Sediments 1 and Water layers) and the average density model (Harkness), with the global relief model ETOPO1 serving as the positional reference, with station spacing of 5 arc minutes. Gravitational potentials were calculated using tesseroids and spherical zonals based on Newton's integral. The mean values of the three models were tested and found to be statistically different. Additionally, the differences in calculated values among the three density models were presented. The effect of RTM on altimetry in Brazil varied between 0 and 2.5 mm, emphasizing its relevance and the necessity of considering it in precision altimetric studies. The developed methodology proved effective and encourages future research on increasing positional and density resolutions, as well as processing RTM with the inclusion of harmonic correction.

Keywords: RTM; Lateral density; Global model; Tesseroids; Zonal.

Resumo: No presente trabalho são apresentadas três representações do comportamento da RTM cobrindo todo território continental brasileiro, utilizando modelos globais de densidade lateral variável UNB_TopoDens e CRUST 1.0 (camadas *Sediments 1* e *Water*) e média (Harkness), e o modelo de relevo global ETOPO1 como referência posicional, com espaçamento entre as estações de 5 minutos de arco. Os potenciais gravitacionais foram calculados utilizando tesseroides e zonais esféricos a partir da integral de Newton. Os três modelos tiveram suas médias testadas e verificou-se serem estatisticamente diferentes. Também foram apresentadas as diferenças dos valores calculados entre os três modelos de densidade. O efeito da RTM sobre a altimetria em território brasileiro, variou entre 0 e 2,5 mm, enfatizando sua importância e consideração em trabalhos altimétricos de precisão. A metodologia desenvolvida mostrou-se eficaz e instiga trabalhos futuros abordando o aumento das resoluções posicionais e de densidades, bem como, o processamento da RTM com a inclusão da correção harmônica.

Palavras-chave: RTM; Densidade lateral; Modelos globais; Tesseroides; Zonal.

Received: 30/12/2024; Accepted: 05/05/2025; Published: 05/05/2025.

1. Introduction

According to Heck and Seitz (2007), the modeling of the effect of different distributions of Earth's topographic masses and their consequent lateral density variations related to the gravitational field is one of the central issues in physical geodesy. The classical Stokes' theory for geoid determination considers the exclusion of topographic masses and their isostatic equilibrium above the boundary surface. In addition to the topo-isostatic gravity reduction, the indirect effect of topographic masses on the gravitational potential must be considered for an accurate geoid determination.

Molodenskii et al. (1962), although originally free of any topographic mass reductions, consider terrain reduction as a correction term in the first-order solution of the so-called Molodenskii series. Currently, the modeling of the local and regional gravitational field incorporates the Residual Terrain Model (RTM), frequently applied within the remove-compute-restore (RCR) technique in the modeling and processing of terrestrial gravitational field data. During the restoration phase of topographic mass effects, their values are influenced by uncertainties in the determination and modeling of lateral density variations (Sjoberg, 2004; Vanicek et al., 2004; Odalović et al., 2018; Wang et al., 2021). High-resolution digital elevation models (DEM) currently available allow for the calculation of gravitational parameters related to the terrain, such as terrain correction, with unprecedented precision (Tsoulis et al., 2009; Hirt et al., 2010; Bucha et al., 2016; Yamazak et al., 2017). In gravimetric reductions, the so-called terrain correction (C_t) represents the gravitational effect of topographic masses, generally considered inadequately (or entirely omitted) in light of the Bouguer reduction. That is, when determining the gravity value on the geoid based on measurement results on Earth's physical surface (Heiskanen and Moritz, 1967; Tenzer et al., 2010). Figure 1 presents the physical surface on which geodetic surveys are conducted, the geoid representing the equipotential of the gravity field—the reference for orthometric heights (H), the Bouguer plateau (which promotes the partial removal of topographic masses above the geoid), and the remaining topographic masses above the geoid (C_{RTM}), representing the residual effect of topographic modeling (RTM).

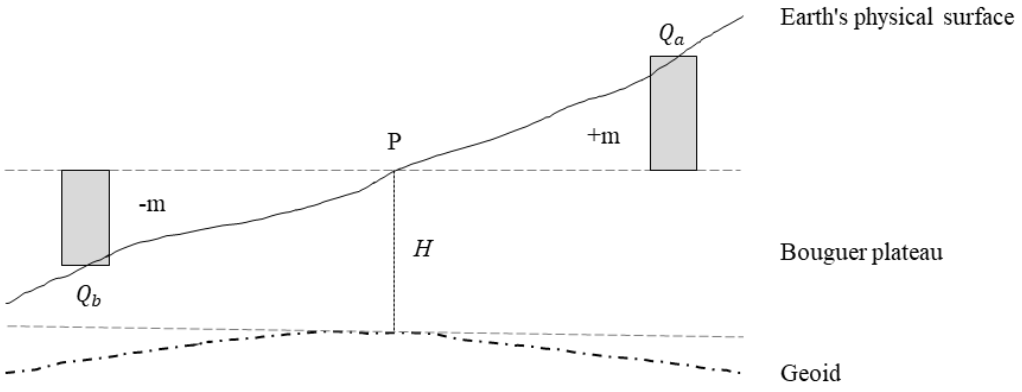

Figure 1 – Elements of terrain correction.
Source: Adapted from Heiskanen and Moritz (1967).

Formula 1 presents the calculation of the terrain correction value (C_t) as a function of its two main components: Bouguer correction (C_B) and residual terrain correction (C_T).

$$C_t = C_B - C_T \tag{1}$$

The Bouguer correction, Formula 2, is classically applied considering a constant lateral density value (ρ=2670 kg/m³), a plateau thickness equal to H, and an application circumference radius of 166.7 km, referring to Hayford's distant zone, assuming the effect of topographic masses between -∞ e +∞, (Gemael, 1999; Vanicek et al. 2001).

$$C_B = 2.\pi.G.\rho.H \tag{2}$$

The gravitational potential v(x,y,z) of a regular prism with homogeneous mass (m), gravitational constant (G), and density (ρ) is described by Formula 3, which presents Newton's integral (Nagy et al., 2000), as shown in Figure 2. Formula 3 calculates the gravitational potential (v) between points P and Q, enabling the first approximation of the RTM effect value (Moritz, 1980). Formula 4 refers to the Euclidean (l_{PQ}).

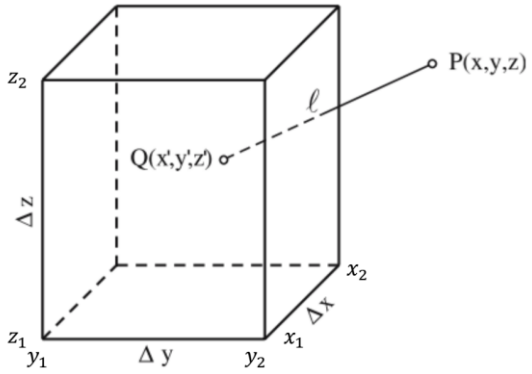

Figure 2 – Geometry of the regular prism.
Source: Adapted from Heck and Seitz (2007).

$$C_T = v(x,y,z) = G.\rho.\int_{z_1}^{z_2}\int_{y_1}^{y_2}\int_{x_1}^{x_2}\frac{dx_{PQ}.dy_{PQ}.dz_{PQ}}{l_{PQ}} \tag{3}$$

$$l_{PQ} = \sqrt{(x'-x)^2 + (y'-y)^2 + (z'-z)^2} \tag{4}$$

$$C_{RTM} = \sum C_T \tag{5}$$

Sánchez et al. (2021) report that the International Association of Geodesy (IAG), in 2015, defined the International Height Reference System (IHRS) as the conventional global altimetric system related to the gravitational field. Current efforts focus on the precise, consistent, and well-defined realization of the IHRS to provide an international standard for the accurate determination of physical coordinates worldwide.

For the materialization of the International Height Reference Frame (IHRF), four main aspects are considered:

a. Methods for determining the physical coordinates of the IHRF;
b. Standards and conventions necessary to ensure consistency between the definition and realization of the reference system;
c. Criteria for designing the IHRF reference network and selecting stations;
d. Operational infrastructure to ensure the reliable and long-term sustainability of the IHRF.

Rodrigues (2022), in his significant contribution to the study of RTM in Brazil, proposes as future research the need to expand studies to additional IHRS stations in Brazil, as well as studies on RTM effects using different approaches and including harmonic corrections (Klees et al., 2022; Yang et al., 2022).

In this context, the present study aims to model and represent RTM values in Brazil using tesseroids and zonal methods (Marotta et al., 2016) along with global altitude and lateral density models.

.

2. Methodology

In the present study, the method developed for determining RTM values employs the spherical tesseroid to calculate the volumes of topographic masses related to the geoid, which produce perturbations in the gravitational potential. The geodetic coordinates of the points (including their orthometric height) are derived from the global altimetric model (ETOPO1), as well as the lateral densities of the topographic masses (UNB_TopoDens, CRUST 1.0, and Harkness). Figure 3 presents the methodological steps applied in this study.

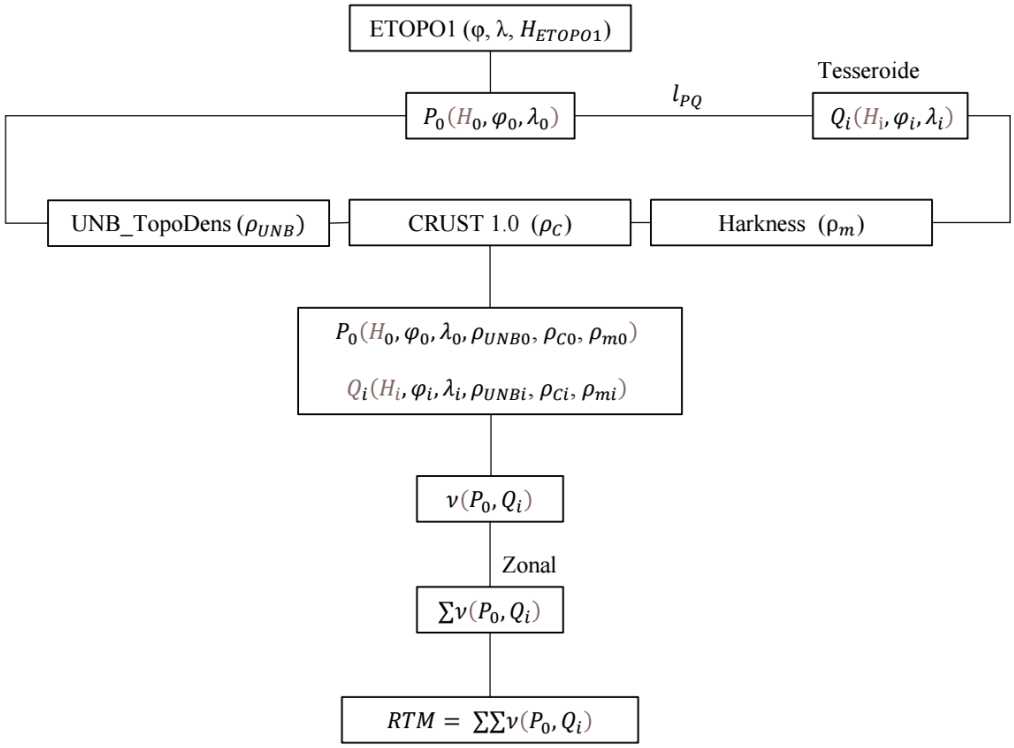

Figure 3 – General schematic of the methodology applied in the present study.
Source: Author (2024).

Figure 4 illustrates the geometry of the spherical tesseroid, applied equidistantly relative to the point where the RTM value is to be determined. The complete set of these tesseroids, varying across 360°, constitutes the spherical zonal, with the RTM being derived from the summation of these zonals. In the same figure, consider two points, P_0 e Q_i. The former represents the location where we seek to determine the gravitational effect induced by the topographic masses above the boundary surface, concentrated at point Q_i. The corresponding geodetic coordinates (in this case, spherical geocentric coordinates) are given by $P_0(r_0, \varphi_0, \lambda_0)$ and $Q_i(r, \varphi, \lambda)$, (Heck and Seitz, 2007).

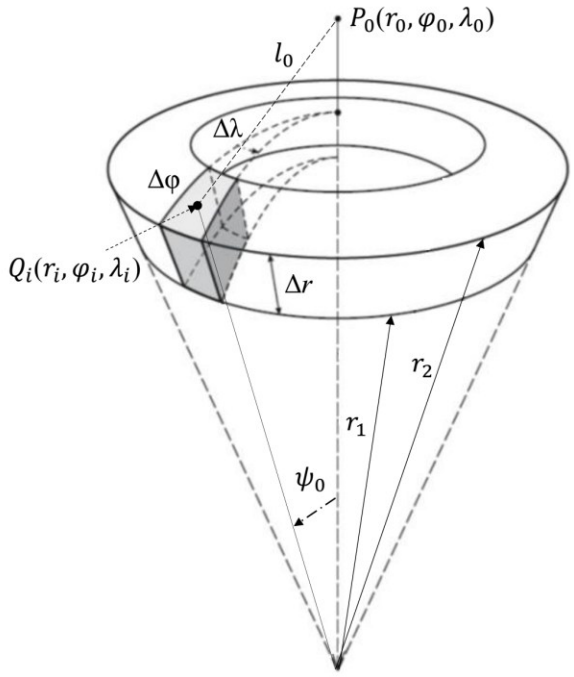

Figure 4 – Tesseroid and zonal.
Source: Adapted from Heck and Seitz (2007).

Assuming that the value of Δr, the difference between the geocentric distances of the physical and boundary surfaces at any given point, can be calculated from r_i or h_i, we have:

$$\Delta r = r_2 - r_1 = \Delta h = h_2 - h_1 \tag{6}$$

r_1, Spherical geocentric distance to the boundary surface;
r_2, Spherical geocentric distance to the physical surface;
h_1, Orthometric height of the boundary surface;
h_2, Orthometric height of the physical surface;

$$P_0(r_0, \varphi_0, \lambda_0) = P_0(h_0, \varphi_0, \lambda_0) \tag{7}$$

$$Q_i(r, \varphi, \lambda) = Q_i(h, \varphi, \lambda) \tag{8}$$

$$r_i = \frac{r_1 + r_2}{2} = h_i = \frac{h_1 + h_2}{2} \tag{9}$$

$$\varphi_i = \frac{\varphi_1 + \varphi_2}{2} \tag{10}$$

$$\lambda_i = \frac{\lambda_1 + \lambda_2}{2} \tag{11}$$

$$\Delta\varphi = \varphi_2 - \varphi_1 \tag{12}$$

$$\Delta\lambda = \lambda_2 - \lambda_1 \tag{13}$$

$$\delta\lambda = \lambda - \lambda_0 \tag{14}$$

ψ_0, Geocentric angle between the directions of P_0 e Q_i;

$$cos\psi_0 = sen\varphi . sen\varphi_0 + cos\varphi . cos\varphi_0 . \cos \delta\lambda \tag{15}$$

l_0, Euclidean distance between P_0 e Q_i;

$$l_0 = \sqrt{r^2 + r_0^2 - 2.r.r_0.cos\psi_0} \tag{16}$$

$v(r, \varphi, \lambda)$, Gravitational potential of the spherical tesseroid with homogeneous density, calculated using Newton's integral;

G, Gravitational constant;

ρ, Density of the tesseroid;

K_{000}, First-order coefficient of the Taylor series;

K_{200}, K_{020}, K_{002}, Second-order coefficients of the Taylor series;

Δ^4, Landau coefficient for terms of fourth order or higher in the Taylor series;

O, Null operator, indicating that terms of fourth order or higher in the Taylor series will be omitted;

$$v(r, \varphi, \lambda) = G.\rho.\Delta r.\Delta\varphi.\Delta\lambda.\left[K_{000} + \frac{1}{24}.(K_{200}.\Delta r^2 + K_{020}.\Delta\varphi^2 + K_{002}.\Delta\lambda^2) + O(\Delta^4)\right] \tag{17}$$

$$K_{000} = \frac{r_0^2.cos\varphi_0}{l_0} \tag{18}$$

$$K_{200} = \frac{r^2.cos\varphi_0}{l_0^5}.\langle 2.l_0^2 - 3.r_0^2.sen^2\psi_0\rangle \tag{19}$$

$$K_{020} = \frac{r_0^2}{l_0^5}.\{-cos\varphi_0.(r^2 + r_0^2).[r^2 + r_0^2 - r.r_0.sen\varphi.sen\varphi_0] + r^2.r_0^2.cos\varphi_0.[sen^2\varphi.(3 - sen^2\varphi_0) - cos^2\varphi.(2 - sen^2\varphi_0).cos^2\delta\lambda] + r.r_0.cos\varphi.(3 - sen^2\varphi_0).[r^2 + r_0^2 - 2.r.r_0.sen\varphi.sen\varphi_0].cos\delta\lambda\} \tag{20}$$

$$K_{002} = -\frac{r.r_0^3.cos\varphi.cos^2\varphi_0}{l_0^5}.\{l_0^2.cos\delta\lambda - 3.r.r_0.cos\varphi.cos\varphi_0.sen^2\delta\lambda\} \tag{21}$$

Figure 5 presents an excerpt from the Global Relief Model (ETOPO1), highlighting part of South America. This model is a set of elevation data referenced to mean sea level (geoid), produced by the National Oceanic and Atmospheric Administration (NOAA). ETOPO1 is a global digital elevation model (DEM) of Earth's surface, with a resolution of 1 arc minute, incorporating both terrestrial topography and ocean bathymetry (NOAA, 2009).

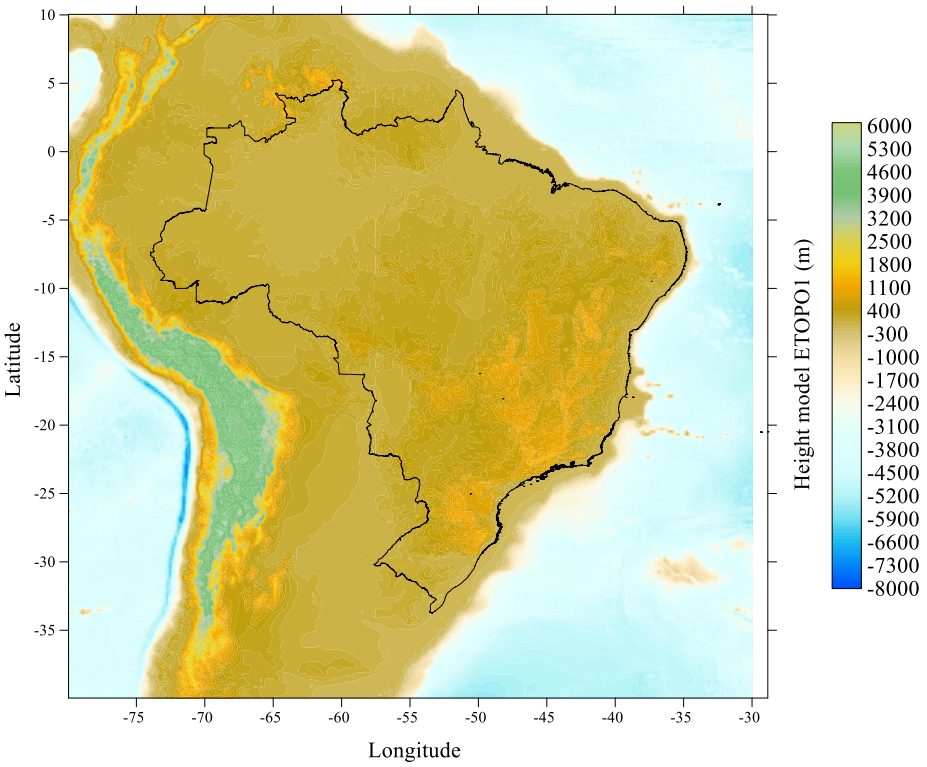

Figure 5 – ETOPO1 altimetry for part of South America.
Source: Author (2024).

The value of 2670 kg/m³ (2.67 g/cm³) for the average density ($\rho_{Harkness}$= ρ_m) of surface rocks in the continental crust is the result of a compilation by William Harkness (1891) of various studies by different authors conducted between 1811 and 1882, aiming to determine the global average density of surface rocks. The value of 2670 kg/m³ is generally assumed based on the density of crystalline surface rocks on continents with granitic composition (granite rock density ranges from 2500 to 2800 kg/m³, with an approximate average of 2670 kg/m³).

According to Sheng et al. (2019), the University of New Brunswick (UNB_TopoDens) density model provides a global model of laterally variable densities in a dense grid, utilizing field-measured data without employing the gravitational inversion method. The final products of this first approximation are topographic density values in three grids of different resolutions (30″, 5′, and 1°), along with their respective standard deviations corresponding to the same resolution intervals. Figure 6 presents the visualization of UNB_TopoDens for part of South America.

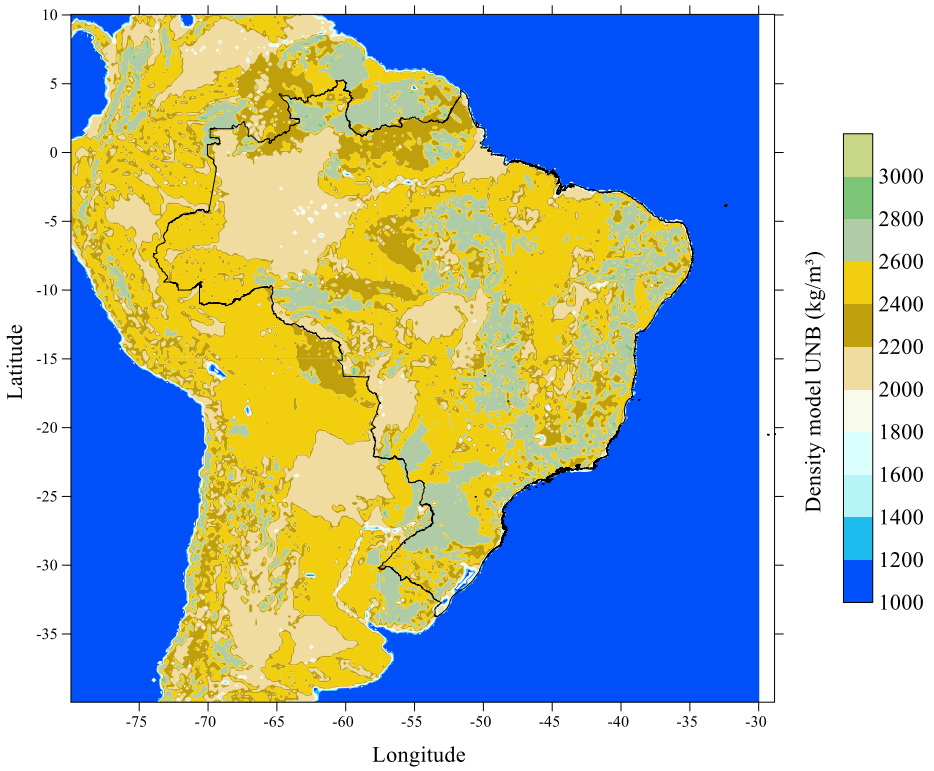

Figure 6 – UNB_TopoDens density model for part of South America.
Source: Author (2024).

CRUST 1.0 is a detailed global model of Earth's crust, developed by Laske et al. (2012) as a replacement for the previous CRUST 2.0 model. With a resolution of 1°x1°, it incorporates significant updates in sediment thickness and other structural layers of the crust, based on topographic and bathymetric data, such as the ETOPO1 model (NOAA, 2009). This model is essential for applications in seismic tomography and geophysical monitoring, providing precise parameters for determining compressional and shear wave velocities, as well as densities for various layers, including water, ice, sediments, and different strata of the crust and upper mantle. CRUST 1.0 is widely used by geophysicists and geologists to enhance the understanding of Earth's internal structure. Figure 7 illustrates the density variations in the Sediments 1 and Water layers of CRUST 1.0 for part of South America.

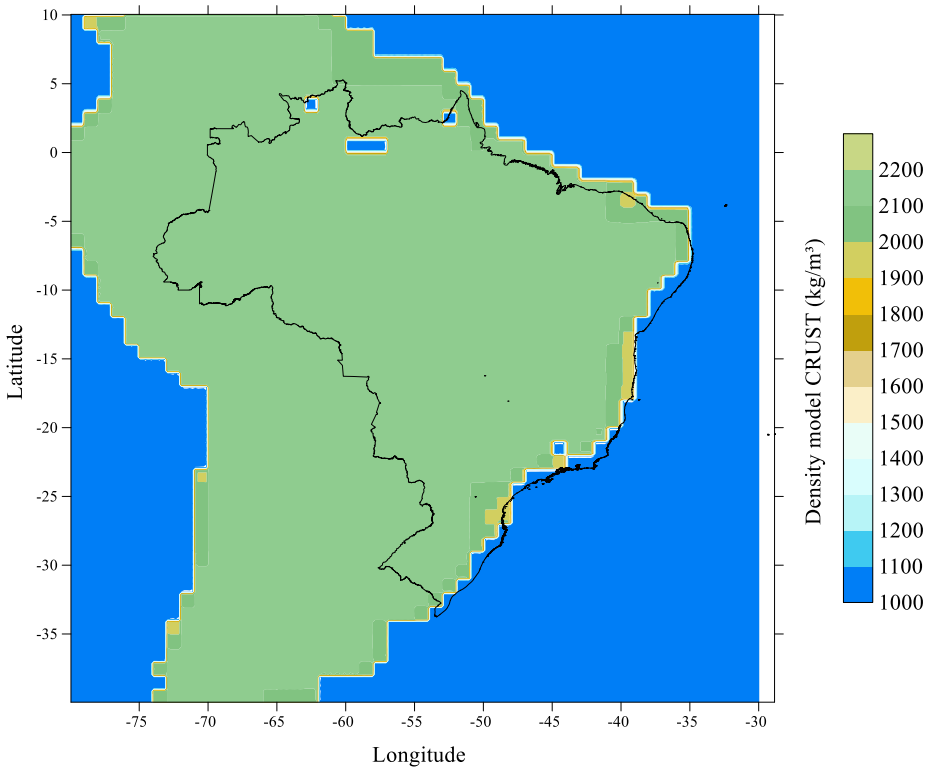

Figure 7 – CRUST 1.0 density model for part of South America.
Source: Author (2024).

3. Results and Discussion

Based on the proposed methodology (the main work steps can be visualized in Figure 4), the first stage involved selecting and organizing data from the global models used: ETOPO1 (Figure 5), UNB_TopoDens (Figure 6), and CRUST 1.0 (Figure 7). Once all the mentioned data were compiled and structured, subsequent steps focused on processing the RTM values for Brazil, using each of the global models of lateral and average densities (Harkness), with a spatial resolution of 5 arc minutes, totaling 101,006 points within the continental Brazilian territory. The RTM values were determined through routines developed in a Matlab environment by the author.

The gravitational potential of the spherical tesseroid with homogeneous density was calculated using Newton's integral, as presented in Formula 17. This formula was applied to a tesseroid with a longitudinal variation of 5 degrees of spherical arc (72 tesseroids for each zonal) and a longitudinal variation of approximately 30 arc minutes (four zonals, each containing 72 tesseroids, totaling 288 tesseroids for each reference point P_0). The reference point for RTM calculation (P_0) considers the points Q_i up to a distance of 210 km.

Figures 8, 9, and 10 illustrate the RTM behavior in Brazil, associated with orthometric heights, meaning the values obtained by dividing the gravitational potential by the respective normal gravity value. These figures represent RTM values corresponding to the global density models UNB_TopoDens, CRUST 1.0, and Harkness. Figures 11, 12, and 13 respectively display the variations in RTM behavior among different models, calculated for the continental Brazilian territory: UNB_TopoDens and Harkness, UNB_TopoDens and CRUST 1.0, and CRUST 1.0 and Harkness.

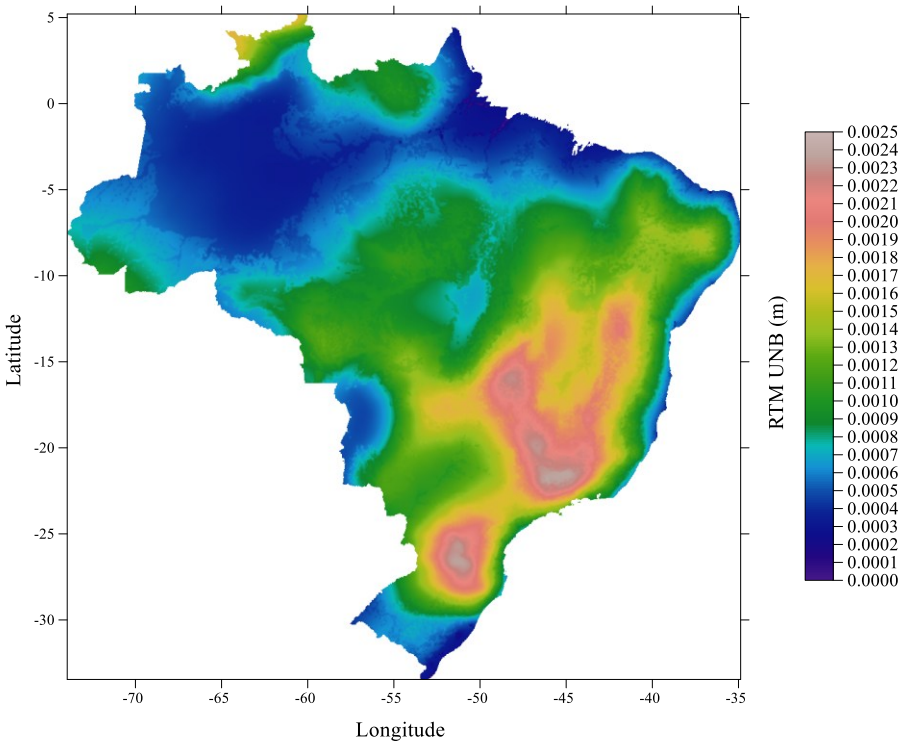

Figure 8 – RTM UNB_TopoDens.
Source: Author (2024).

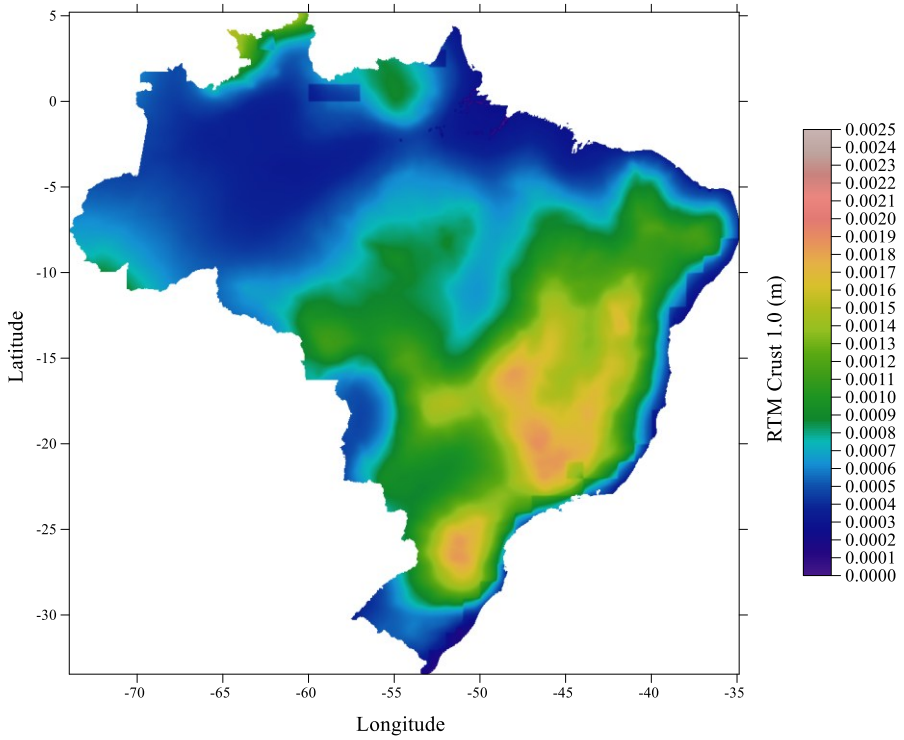

Figure 9 – RTM CRUST 1.0.
Source: Author (2024).

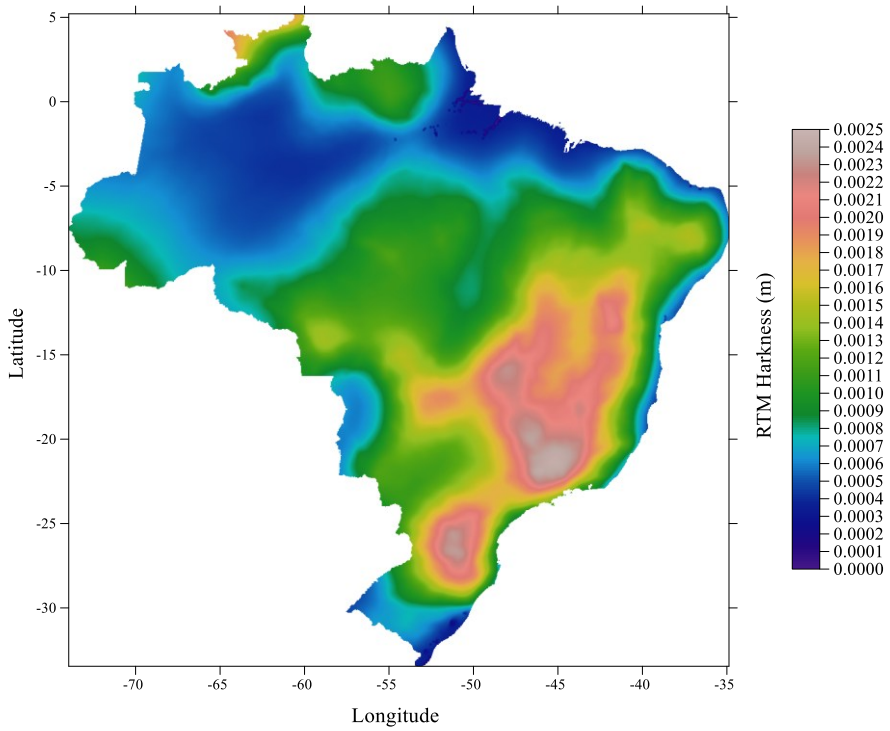

Figure 10 – RTM Harkness.
Source: Author (2024).

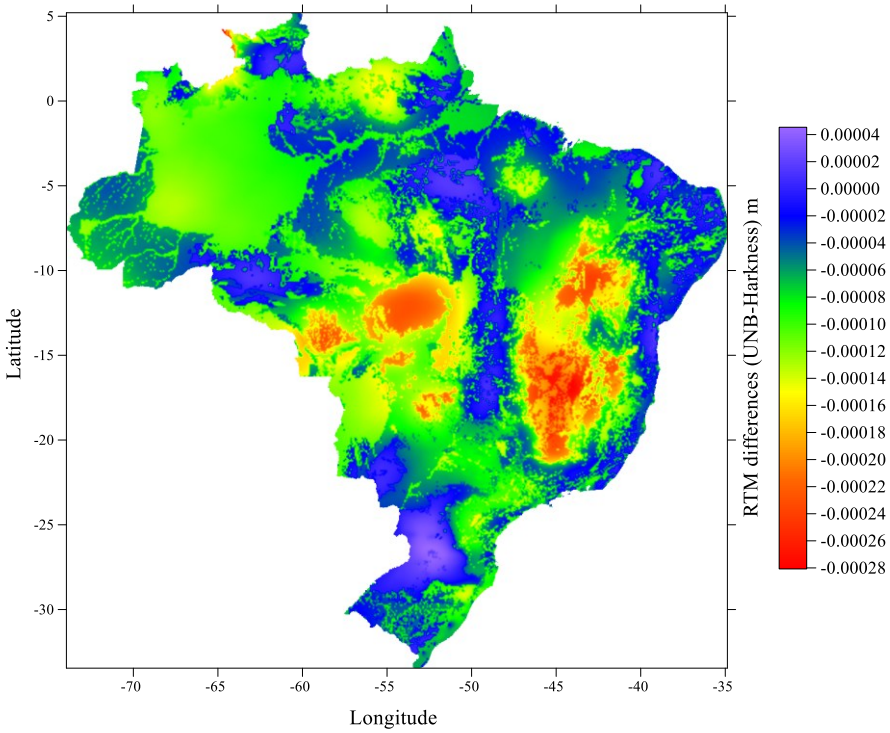

Figure 11 – Differences between RTM UNB_TopoDens and RTM Harkness.
Source: Author (2024).

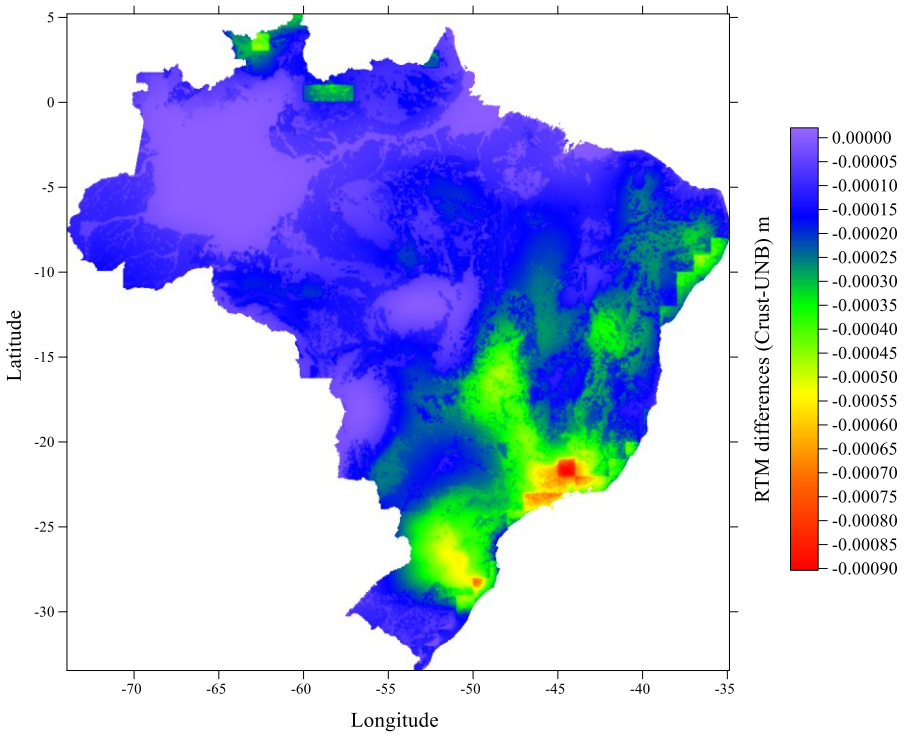

Figure 12 – Differences between RTM UNB_TopoDens and RTM CRUST 1.0. Source: Author (2024).

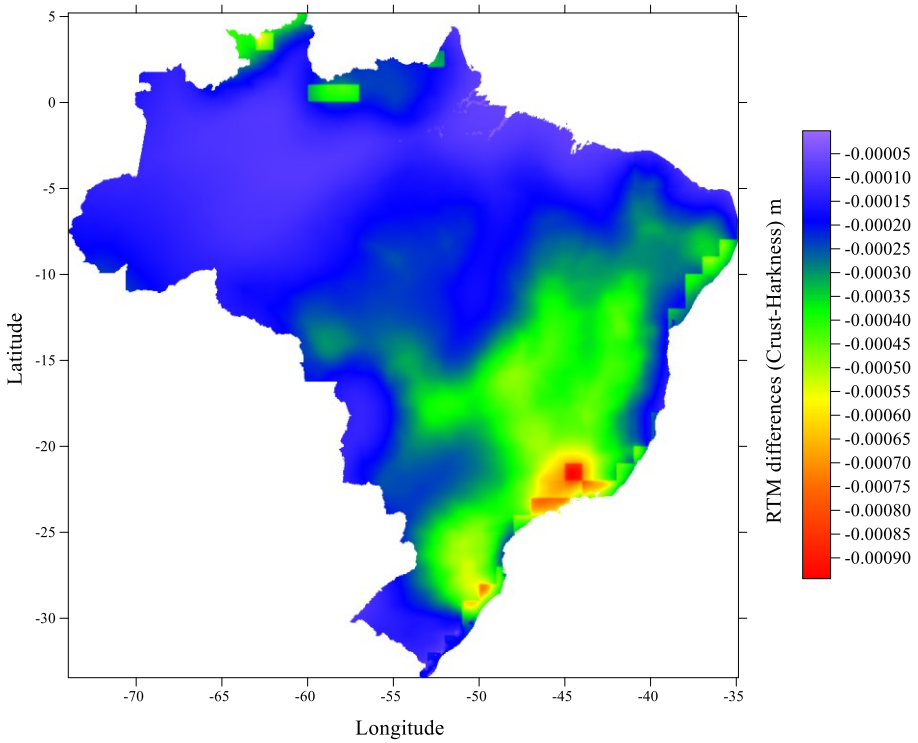

Figure 13 – Differences between RTM CRUST 1.0 and RTM Harkness. Source: Author (2024).

Statistical analyses began with the calculation of correlation and variance-covariance matrices among the global models. In Table 1, we observe correlations exceeding 90% between the RTM values computed using different global density models and orthometric height, and correlations above 98% among the RTM values themselves, confirming the strong dependency between the variables through the mathematical model applied. In conjunction with the variance-covariance matrix (Table 2), we find that the UNB_TopoDens and Harkness models, associated with altitude variation, exhibit greater sensitivity compared to the CRUST 1.0 model. It is important to note that in this study, only the Sediments 1 and Water layers of CRUST 1.0 were used in the calculation of the respective density values.

Table 1 – Correlation matrix between H and global density models.

	H	rtmUNB	rtmC	rtmH
H	1			
rtmUNB	0.914	1		
rtmC	0.904	0.986	1	
rtmH	0.916	0.994	0.994	1

Source: Author (2024).

Table 2 – Variance-covariance matrix between H and global density models.

	H	rtmUNB	rtmC	rtmH
H	68,668.24			
rtmUNB	0.118524	2.45E-07		
rtmC	0.093725	1.93E-07	1.57E-07	
rtmH	0.121732	2.5E-07	2E-07	2.57E-07

Source: Author (2024).

The frequency histograms in Figures 14, 15 and 16, show that the RTM variation amplitudes in Brazil ranged between 0 and 2.5 mm for the UNB_TopoDens and Harkness models, and between 0 and 2.0 mm for the CRUST 1.0 model. In all three models, the highest frequencies are between 0.5 and 1.0 mm, accounting for more than 40% of the total.

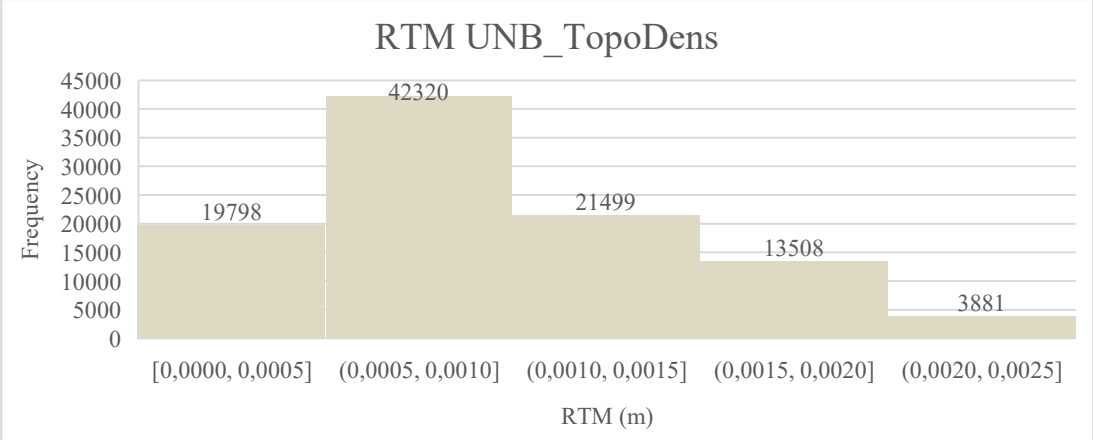

Figure 14 – Frequency histogram of RTM UNB_TopoDens.
Source: Author (2024).

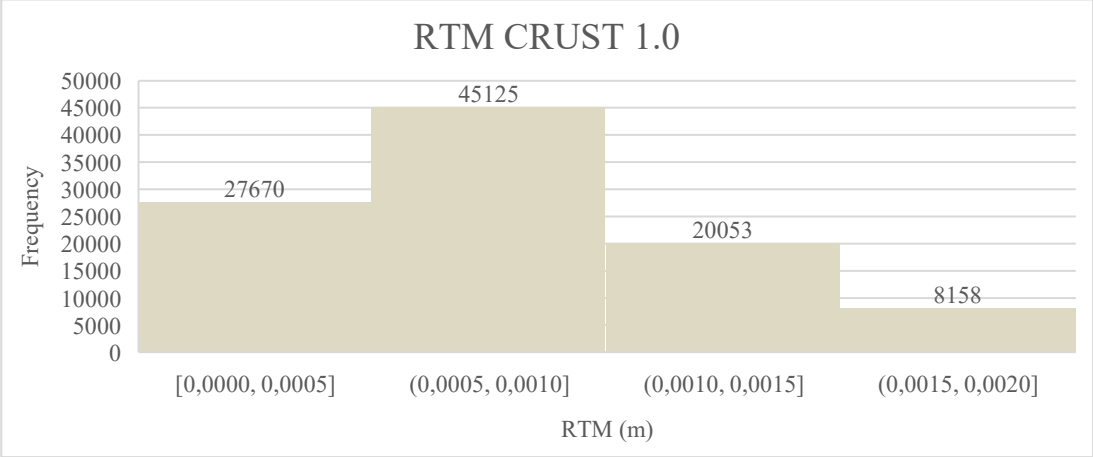

Figure 15 – Frequency histogram of RTM CRUST 1.0.
Source: Author (2024).

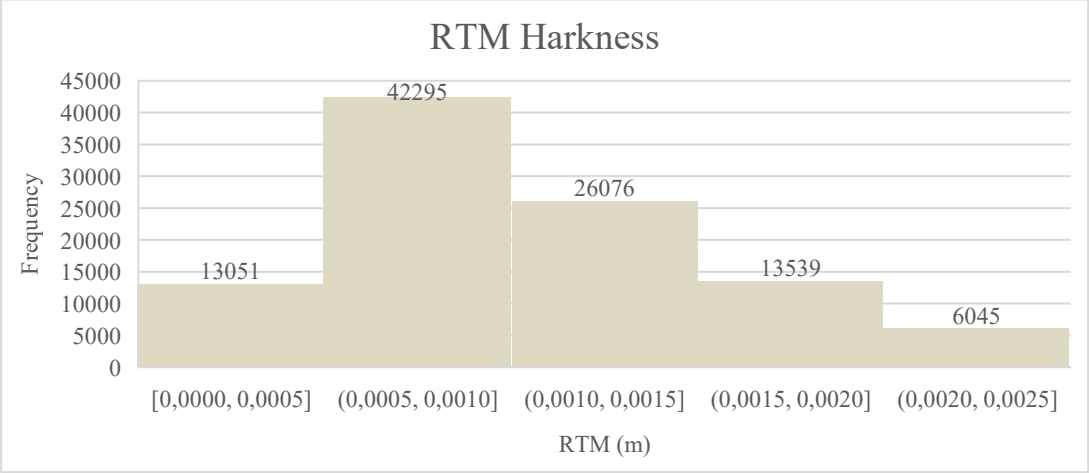

Figure 16 – Frequency histogram of RTM Harkness.
Source: Author (2024).

The analysis of variance was applied to evaluate whether the mean values associated with global and average density values are statistically equal (null hypothesis) or if at least one of the tested means is statistically different (alternative hypothesis). Table 3 presents the descriptive statistical summary related to the ANOVA (Analysis of Variance) test, which serves as the basis for hypothesis testing in Table 4. From Table 4, we observe that the critical value (at a 5% significance level) was significantly exceeded by the sample value. Additionally, the p-statistic is lower than the significance level of the test, both strongly indicating a rejection of the null hypothesis.

Table 3 – Statistical Summary (ANOVA).

Group	*Count*	*Sum (m)*	*Mean (m)*	*Variance (m²)*
rtmUNB	101,006	98.417671	0.00097437	2.4513E-07
rtmCRUST	101,006	83.081041	0.00082254	1.5663E-07
rtmHarkness	101,006	106.68167	0.00105619	2.5726E-07

Source: Author (2024).

Table 4 – ANOVA Summary.

Source of variation	*SQ*	*gl*	*MQ*	*F*	*P-value*	*F critical*
Between groups	0.00283975	2	0.00141988	6,463.64084	0	2.99576189
Whitin groups	0.06656365	303,015	2.1967E-07			
Total	0.0694034	303,017				

Source: Author (2024).

Since the ANOVA test only indicates the existence of at least one mean that is statistically different from the others, the parametric Tukey test was applied. This test calculates the minimum significant difference (MSD) factor and applies it to the differences between the means through pairwise comparison. Table 5 presents the results of the Tukey test for the RTM means calculated for Brazil, associated with global models and the average density of topographic masses. By pairing the models, the analysis of statistical equality or difference in RTM means, at a 5% significance level, examines the result of the |ΔM/MSD| factor. If this value is greater than 1, the compared means are statistically different. In this case, we confirm that the RTM means associated with each density model are statistically different from each other.

Table 5 – Summary of the Tukey Test.

Contrast (RTM)	Mean Difference (ΔM)	DMS	|ΔM/DMS|
UNB-CRUST	0.000151839	4.88136E-06	31.10583426
UNB-Harkness	-8.18169E-05	4.88136E-06	16.76108684
CRUST-Harkness	-0.000233656	4.88136E-06	47.8669211

Source: Author (2024).

4. Final Considerations

This study has effectively and uniquely presented the behavior of RTM (with emphasis on altimetry) in the continental portion of Brazil. The analysis was based on positional ETOPO1 data and density values at a resolution of 5' × 5', totaling 101,006 points, considering the effect of Hayford zones up to 210 km. The global lateral density models (UNB_TopoDens and CRUST 1.0) and the average density model (Harkness) were individually applied and compared to determine RTM values, employing Newtonian integration applied to tesseroids and spherical zonal components. Numerically, in this study, the RTM in Brazil varied between 0 and 2.5 mm, highlighting its relevance to both national and global altimetric systems. Further refinements of the mathematical model such as the incorporation of harmonic corrections, high-resolution positional and density data should be explored in future studies. Additionally, accuracy assessments of various data groups and adjustment models should be considered for subsequent research.

References

Bucha, B., Janák, J.; Papčo, J.; Bezděk. A. High-resolution regional gravity field modelling in a mountainous area from terrestrial gravity data. *Geophysical Journal International* v.207, 949–966, 2016.

Gemael, C. *Introdução à Geodésia Física*. Curitiba, Brasil: Editora da Universidade Federal do Paraná. 1999. 304p.

Harkness, W. Solar parallax and its related constants, including the figure and density of the Earth. *Government Printing Office,* 1891.

Heck, B.; Seitz. K. A comparison of the tesseroid, prism and point-mass approaches for mass reductions in gravity field modelling. *Journal of Geodesy*, v.81, 121–136, 2007.

Heiskanen, W.A., Moritz, H. *Physical geodesy*. San Francisco, USA: Ed. Freeman, 1967. 364p.

Hirt, C.; Featherstone, W.E.; Marti, U. Combining EGM2008 and SRTM/DTM2006.0 residual terrain model data to improve quasigeoid computations in mountainous áreas devoid of gravity data. *Journal of Geodesy*, v.84, 557–567, 2010.

Klees, R.; Seitz, K.; Slobbe. D.C. The RTM harmonic correction revisited. *Journal of Geodesy*, v.96, 39p, 2022.

Laske, G., Masters, G., Ma, Z., Pasyanos, M.E. CRUST1.0: an updated global model of Earth's CRUST. *Geophysical Research Abstract*. EGU2012–37431, 2012.

Marotta, A. M.; Barzaghi, B. A new methodology to compute the gravitational contribution of a spherical tesseroid based on the analytical solution of a sector of a spherical zonal band. *Journal of Geodesy*, v.91, 1207–1224, 2017.

Molodenskii, M.S.; Eremeev, V.F.; Yurkina, M.I. *Methods for Study of the External Gravitational Field and Figure of the Earth*. Jerusalem, Israel: Israeli Programme for the Translation of Scientific Publications, 1962. 264p.

Moritz, H. *Advanced physical geodesy*. Karlshure, Germany: Ed. Wichmann, 1980. 500p.

Nagy, D.; Papp, G.; Benedek, J. The gravitational potential and its derivatives for the prism. *Journal of Geodesy*, v.74, 552–560, 2000.

NOAA. National Geophysical Data Center. 2009: *ETOPO1 1 Arc-Minute Global Relief Model*. Disponível em https://www.ngdc.noaa.gov/mgg/global/relief/ETOPO1/data/ Acesso em: 08/12/2024.

Odalović, O.R.; Grekulović, S.M; Starcević, M.; Nikolić, D.; Drakul, M.S.T.; Joksimović, D. Terrain correction computations using digital density model of topographic masses. *Geodetsky Vestnik*, v.62, n.1, 79-97, 2018.

Rodrigues, T. L. A contribution for the study of RTM effect in height anomalies at two future IHRS stations in Brazil using different approaches, harmonic correction, and global density model. *Journal of Geodetic Science*, v.12, 75-91, 2022.

Sánchez, L.; Agren, J.; Huang, J.; Wang, Y.M.; Makinen, J.; Pail, R. Strategy for the realization of the International Height Reference System (IHRS). *Journal of Geodesy*, v.95(33), 1–33, 2021.

Sheng, M.B., Shaw, C., Vanícek, P., Kingdon, R.W., Santos, M., Foroughi, I. Formulation and validation of a global aterally varying topographical density]model. *Tectonophysics*. v.672, 45–60, 2019.

Sjöberg, L. The effect on the geoid of lateral topographic density variations. *Journal of Geodesy*, v.78, 34–39, 2004.

Tenzer, R.; Hamayun, Z.; Prutkin, I. A comparison of various integration methods for solving Newton's integral in detailed forward modelling. In: Mertikas, S. (eds) *Gravity, Geoid and Earth Observation. International Association of Geodesy Symposia* 135. Berlin, Heidelberg: Springer. 2010.

Tsoulis, D.; Novák, P.; Kadlec, M. Evaluation of precise terrain effects using high-resolution digital elevation models. *Journal of Geophysical Research*, v.114, B02404, 2009.

Vanicek, P.; Novák P.; Martinec, Z. Geoid, topography, and the Bouguer plate or shell. *Journal of Geodesy*, v.75(4), 210–215, 2001.

Vanicek, P.; Tenzer, R.; Sjöberg, L.E.; Martinec, Z.; Featherstone, W.E. New views of the spherical Bouguer gravity anomaly. *Geophysical Journal International*, v.159, 460–472, 2004.

Wang, Y. M.; Sanchez, L.; Ågren, J.; Huang, J.; Forsberg, R.; Abd-Elmotaal, H.A. Colorado geoid computation experiment – overview and summary. *Journal of Geodesy*, v.95. 2021.

Yamazaki, D.; Ikeshima, D.; Tawatari, R.; Yamaguchi, T.; O'Loughlin, F.; Neal, J.C. A high accuracy map of global terrain elevations. *Geophysical Research Letters*, v.44, 5844–5853, 2017.

Yang, M.; Hirt, C.; Wu, B.; Deng, X.; Tsoulis, D.; Feng, W. Residual Terrain Modelling: The Harmonic Correction for Geoid Heights. *Surveys in Geophysics*, v.43, 1201–1231, 2022.